Applied Catalysis B: Environmental 88 (2009) 50–58

Contents lists available at ScienceDirect

Applied Catalysis B: Environmental

journal homepage: www.elsevier.com/locate/apcatb

The direct–indirect kinetic model in photocatalysis: A reanalysis of phenol and formic acid degradation rate dependence on photon flow and concentration in TiO_2 aqueous dispersions

J.F. Montoya [a], J.A. Velásquez [a], P. Salvador [b,c,1,*]

[a] Grupo de Procesos Fisicoquímicos Aplicados, Departamento de Ingenieria Química, Universidad de Antioquia, Medellín, Colombia
[b] Departament de Ciències Matemàtiques i Informàtica, Universitat de les Illes Balears, E-07071 Palma de Mallorca, Spain
[c] Instituto de Electroquímica, Universidad de Alicante, Spain

ARTICLE INFO

Article history:
Received 17 July 2008
Received in revised form 10 September 2008
Accepted 19 September 2008
Available online 18 October 2008

Keywords:
TiO_2 photocatalysis
Phenol
Formic acid
Photooxidation kinetics
Direct–indirect model
Langmuir–Hinshelwood model

ABSTRACT

Literature data concerning TiO_2 photocatalytic oxidation of two model organic substrates, phenol and formic acid, are shown to be incompatible with the behavior predicted by the Langmuir–Hinshelwood (L–H) kinetic model. These data are reanalyzed in detail from a kinetic/mechanistic point of view to the light of the direct–indirect (D–I) model (D. Monllor-Satoca, R. Gomez, M. Gonzalez-Hidalgo, P. Salvador, Catal. Today 129 (1–2) (2007) 247), developed as an alternative to the L–H model. Two interfacial charge transfer mechanisms are considered by the (D–I) model: the indirect transfer (IT) mechanism, which is concerned with the adiabatic transfer of holes trapped at TiO_2 terminal oxygen ions to dissolved substrate species, and the direct transfer (DT) mechanism dealing with the inelastic transfer of free holes to specifically adsorbed substrate species. While IT is the only mechanism taking place in the absence of specific adsorption, both DT and IT mechanisms actuate simultaneously under specific adsorption, although DT prevails on IT at high enough UV illumination intensity. On the experimental basis that in aqueous solution phenol is not specifically adsorbed on TiO_2, it is shown that the experimental photodegradation rate dependence on photon flux (ρ) and phenol concentration (C) is not compatible with a Langmuir type expression, but can be fitted by the photooxidation rate expression $(dC/dt) = [(aC)^2 + 2k_0a\rho C]^{1/2} - aC$, as predicted by the D–I model for IT, where a is an experimental parameter involving the rate constants for electron–hole recombination and transfer of photogenerated electrons and holes at the semiconductor–electrolyte interface. An apparent dependence of a on ρ and C is observed experimentally. Two possible hypothesis are invoked in order to explain this behaviour:a shift of the TiO2 energy levels, due to an accumullation of electric charge at the semiconductor surface, and/or the partial contribution of inelastic DT of holes to incipiently adsorbed phenol species. Evidence is given that the photooxidation rate of formic acid, which is shown to be specifically adsorbed on TiO_2 in the presence of water, depends linearly on ρ, even at high enough photon flux values, as predicted by the D–I model when DT prevails on IT, but in contradiction with the behavior predicted by the L–H model.

1. Introduction

The kinetic study of the photocatalytic oxidation of water dissolved organic compounds play an important role both from a practical and fundamental point of view. This kinetics has been generally regarded to be based on a Langmuir–Hinshelwood (L–H) first-order equation of the initial reaction rate vs. initial substrate concentration [1–8]. As claimed by Emeline et al., the nearly universal robotic application of the L–H kinetic model to interpret the kinetic data of heterogeneous photoreactions constitutes a dogma in photocatalysis [3].

In the classical paper by Turchi and Ollis [5], four possible mechanisms for the TiO_2 photocatalytic degradation of organic water contaminants, all based on hydroxyl radical attack of the organic reactant, were suggested: (1) OH radicals adsorbed at terminal Ti^{IV} atoms react with $(RH_2)_{ads}$, specifically adsorbed substrate species; (2) free (non-adsorbed) OH radicals react with $(RH_2)_{ads}$ species; (3) adsorbed OH radicals react with non-adsorbed

* Corresponding author at: Departament de Ciències Matemàtiques i Informàtica, Universitat de les Illes Balears, E-07071 Palma de Mallorca, Spain.
E-mail address: dmipss9@uib.es (P. Salvador).
[1] On leave from the Instituto de Catálisis y Petroleoquímica, CSIC, Spain.

0926-3373/$ – see front matter © 2008 Elsevier B.V. All rights reserved.
doi:10.1016/j.apcatb.2008.09.035

organic species (Elley–Rideal (E–R) mechanism); (4) free OH radicals react with dissolved organic molecules. Reaction of valence band (VB) free holes with specifically adsorbed contaminant species were not considered by the authors. Turchi and Ollis [5] conclude that in all considered four mechanisms a Langmuir type law described by the expression:

$$\frac{dC}{dt} = \frac{k_{obs}K_L C}{1 + K_L C} \quad (1)$$

is obtained for the degradation rate (dC/dt), where the apparent Langmuir adsorption constant, K_L, is predicted to be photon flux independent, while the apparent photoreaction rate, k_{obs}, appears to be proportional to ρ for low photon flux and proportional to $\rho^{1/2}$ for high photon flux, indicating a transition region between "low" and "high" illumination intensity [5]. However, it must be noted that contrasted experimental evidence about this transition is not present in the literature. On the other hand, these predictions were obtained on the basis of the following improper assumptions [5]: (1) direct band-to-band recombination is the main electron–hole recombination mechanism, a forbidden mechanism for high bandgap semiconductors like TiO_2 [3]; (2) the concentration of photogenerated holes is identical to the concentration of photogenerated electrons, which is in general uncertain [9]; (3) direct transfer of valence band free holes to adsorbed substrate species is considered to be insignificant, something incorrect as shown previously [9,10] and discussed here.

More recently, in a kinetic study of phenol photooxidation, Serpone and co-workers [2] proposes Eq. (2) as a modification of the Langmuir expression

$$\frac{dC}{dt} = \frac{\alpha\rho C}{\beta\rho + \gamma C} \quad (2)$$

where α, β and γ are experimental constants without defined physical meaning and independent of ρ and C. Interestingly, according to (2), $(dC/dt) \approx (\alpha/\beta)C$ for $\rho\beta \gg \gamma C$ and $(dC/dt) \approx (\alpha/\gamma)\rho$ for $\rho\beta \ll \gamma C$ Eq. (2) is obtained by Emeline et al. on the basis of the following assumptions: (a) surface-bound $OH^\bullet$ radicals, photogenerated via trapping of VB free holes (h_f^+) by hydroxyl groups and/or water molecules adsorbed on terminal Ti atoms, are the only active species in the photocatalytic oxidation process; (b) photogenerated surface-bound $OH^\bullet$ radicals are able to attack phenol molecules, independently on whether they are specifically adsorbed (L–H mechanism) or non-adsorbed (E–R mechanism), which means that Eq. (1) is compatible with both the L–H and the E–R mechanism; (c) surface-bound $OH^\bullet$ radicals are annihilated via recombination with conduction band (CB) electrons. However, the authors do not take into account the following premises: (a) if specific adsorption is assumed, the attack of phenol species by VB free holes, rather than by surface-bound OH radicals, should be the prevailing interfacial charge transfer mechanism [9,10]; (b) in the absence of extra dissolved, oxidized species, the reduction of dissolved oxygen molecules with CB electrons is a fundamental step to be considered necessarily in the kinetic analysis of the oxidative mechanism; the reduction rate of dissolved O_2 with CB electrons must compensate the oxidation rate of dissolved substrate species with VB holes in order to keep the constraint of semiconductor electroneutrality [11].

If Eq. (2) is identified with Eq. (1), as assumed by Emeline et al. [2] it should be $k_{obs} = (\alpha/\gamma)\rho$ and $K_L = (\gamma/\beta)(1/\rho)$ (i.e., $K_L^{-1} = (\beta/\gamma)\rho$), which contradicts the L–H model premise of a photon flux independent Langmuir constant under equilibrated adsorption/desorption of reactants. As pointed out by Ollis [8], this apparent incongruence can be avoided if the reactant adsorption–desorption equilibrium existing in the dark is assumed to be broken under illumination (pseudo-steady state hypothesis). However, as we will shown below, Ollis approach is not justified in the kinetic analysis of phenol photooxidation, as far as Eq. (1) is not compatible with the observed photodegradation behavior observed by Emeline et al. [2]. Furthermore, the pseudo-steady state hypothesis fails to explain the experimental fact that K_L under illumination is higher than the adsorption equilibrium constant in the dark.

As an alternative approach to the L–H model for analyzing photocatalytic kinetic data, we have developed recently the direct–indirect (D–I) model on the basis of the degree of interaction of the solute organic species to be photooxidized with the semiconductor surface [9,10].The D–I model approach spreads the generalized use in photocatalysis of classical concepts like direct, indirect, adiabatic and inelastic, which are absent in the L–H model, as basic tools for describing the transfer of charge at the semiconductor–electrolyte interface [12]. In contraposition with the L–H model, where photooxidation kinetics appears to be independent of the photooxidation mechanism [5], two types of interfacial hole transfer mechanisms, leading to different kinetics behavior, are considered by the D–I model. For strong electronic interaction of dissolved substrate species with the semiconductor surface (specific adsorption), interfacial transference of charge takes place via a mixture of adiabatic, indirect transfer (IT) of surface trapped holes to dissolved substrate species and inelastic, direct transfer (DT) of VB free holes to substrate species bound to terminal Ti atoms. In contrast, for weak enough electronic interaction of dissolved substrate species with the TiO_2 surface (total absence of specific adsorption), photooxidation is assumed to take place exclusively via an IT mechanism involving surface trapped holes (photogenerated free holes trapped at O_s^{2-} terminal ions) [13]. However, DT coexist with IT in all cases where specific adsorption, even if small, takes place to some extent. In general, the IT mechanism prevails on the DT mechanism for low enough photon flux, while DT prevails on IT for high enough illumination intensity, whenever the photooxidation rate is not limited by diffusion of dissolved substrate species. A photon flux independent photooxidation quantum yield ($(dC/dt) \propto \rho$ for any C) is predicted in the last case, in contradiction with the behavior predicted by the L–H model, where $(dC/dt) \propto \rho$ only for low enough photon flux and high enough substrate concentration [5]. Unlike the L–H model, the D–I model provides a well defined physical meaning to the kinetic constants involved in the intervening, primary interfacial charge transfer reactions [9,10].

In order to verify the applicability of the D–I model, we have paid attention to the photodegradation of two model organic compounds, phenol (Ph) [2] and formic acid (FA) [14], by performing a detailed kinetic reanalysis of their photooxidation kinetics from experimental data existing in the literature. The first question posed by the D–I model concerns the degree of interaction (specific adsorption) of the organic substrate with the TiO_2 surface. While Ph is known to be poorly adsorbed [15,16] FA strongly interact with the TiO_2 surface [16]. This behavior is confirmed in Fig. 1, which allows to compare the ATR-IR spectra of phenol and formic acid aqueous solution, both in presence and absence of a nanostructured TiO_2 thin film and without simultaneous UV illumination. The dramatic intensity increase of the bands corresponding to formic acid in the presence of the nanostructured TiO_2 thin film provides evidence of their specific adsorption. In contrast, the fact that the intensity of the ATR-IR bands of Ph remains practically unchanged in the presence of the TiO_2 thin film points out to the absence of specific adsorption (Ph dissolved species are not able to replace specifically adsorbed water species). A similar conclusion has been reached by different authors [17–19]. It is not our objective here to correlate the

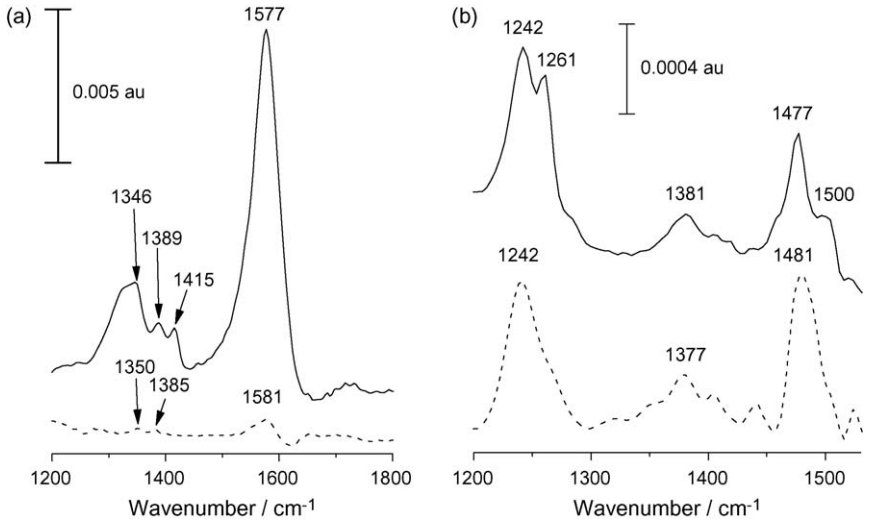

Fig. 1. ATR-IR spectra for (a) 0.01 M formic acid (pH 3.5) in the presence (–) and in the absence (- - - - -) of a 5 μm-thick nanostructured TiO_2 (P25) film, the appearing bands being assigned to 1346 cm^{-1}, symmetric COO group stretching, 1389 cm^{-1}, H–C═O group bending and 1577 cm^{-1} asymmetric COO stretching; (b) 0.01 M phenol (pH 3.5) in the presence (–) and the absence (- - - - -) of a 5 nm-thick nanostructured TiO_2 (P25) film. The bands for the solution spectrum can be assigned as follows [80]: 1242 cm^{-1}, C–O stretching, 1381 cm^{-1} in plane C–O–H bending and 1477 and 1500 cm^{-1}, aromatic ring C–C stretching. In all cases the supporting electrolyte was 0.1 M $NaClO_4$.

observed small shifts of ATR-IR peaks with adsorption mechanisms. These conclusions remain valid when the experiments are performed under simultaneous UV irradiation of the TiO_2 thin films in contact with phenol and formic acid aqueous solutions, as no evidence exists that ATR-IR spectra become appreciably modified. It can be expected, therefore, that FA and Ph should be good candidates for testing the D–I model: while DT should be the prevailing mechanism in the photooxidation of formic acid, as it is specifically adsorbed on TiO_2, IT should prevail on DT in the photodegradation of phenol, as it is scarcely or non adsorbed. Evidence will be given here that the D–I model satisfactorily explains the photooxidation kinetics of both organic compounds. Furthermore, we will demonstrate that a kinetics defined by a L–H type expression, like Eq. (1) and/or Eq. (2), even if compatible with experimental data concerning the photooxidation of specifically adsorbed substrate species (e.g., formic acid) under high illumination intensity conditions, cannot be applied to the photooxidation of dissolved substrate species, like Ph, that can be photooxidized without being previously adsorbed, as they do not interact electronically with the semiconductor surface (E–R model).

2. Photocatalytic phenol oxidation: a kinetic reanalysis of literature experimental data

Among wastewater treatment techniques for phenol elimination, TiO_2 assisted photocatalytic degradation under UV irradiation has attracted the attention of many researchers during the last 20 years [1–4,8,20–66]. To our knowledge, the only detailed kinetic study of the photooxidative degradation of phenol is due to Emeline et al. [2], who performed a careful analysis of the initial photooxidation rate dependence on the incident photon flux for variable phenol concentration, and on the phenol concentration for variable photon flux. Through this study, the authors claim to have found an experimental dependence of the initial photooxidation rate on ρ and C, in agreement with Eq. (2). Fig. 2 reproduces Emeline et al. experimental results concerning the initial photodegradation rate dependence on phenol concentration for different values of the relative illumination flux, ρ/ρ_0 [2]. A reasonable good fitting of Eq. (1) to the experimental points is apparently obtained. Fig. 3 reproduces the dependence of both constants k_{obs} and K_L on the photon flux according to the best fitting of the experimental points of Fig. 2 to Eq. (1). As assumed by the authors, k_{obs} depends linearly on the photon flux. However, as shown in the plot of K_L^{-1} on ρ/ρ_0 of Fig. 4, a clear deviation of the linear dependence of either K_L on ρ_0/ρ or K_L^{-1} on ρ/ρ_0, assumed by the authors, is evident for $\rho/\rho_0 \geq 0.5$.

Eq. (2) can be transformed into Eq. (3)

$$\left(\frac{dC}{dt}\right)^{-1} = \frac{\beta}{\alpha}\frac{1}{C} + \frac{\gamma}{\alpha}\frac{1}{\rho} \quad (3)$$

which indicates that both plots of $(dC/dt)^{-1}$ vs. C^{-1} for ρ = constant and $(dC/dt)^{-1}$ vs. ρ^{-1} for C = constant, must be linear with constant slopes of (β/α) and (γ/α), respectively. However, as shown in Fig. 5, the plot of $(dC/dt)^{-1}$ vs. C^{-1} obtained from the experimental data of Fig. 2, shows that expected linearity is lost for low enough C^{-1} values; in fact, an inflexion point is evident in curves 2 to 7 for $(C)^{-1} \leq 4.0\ mM^{-1}$ and $\rho \geq 1.3 \times 10^{16}\ cm^{-2}\ s^{-1}$, indicating that

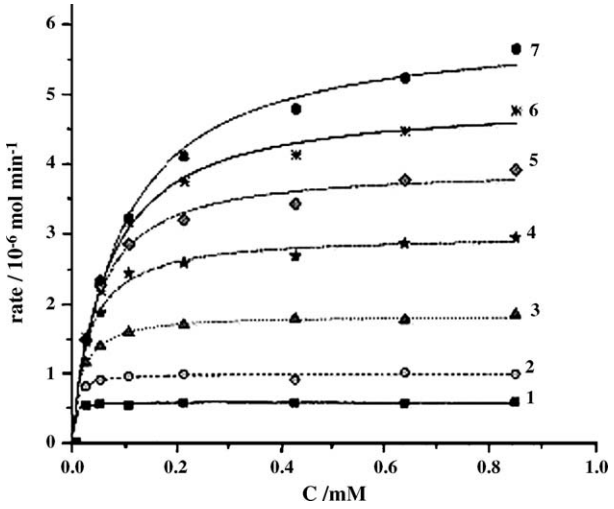

Fig. 2. Initial phenol photodegradation rate dependence on phenol concentration at different photon flux of actinic light at 365 nm: (1) $\rho = 0.06\rho_0$, (2) $\rho = 0.12\rho_0$, (3) $\rho = 0.29\rho_0$, (4) $\rho = 0.50\rho_0$, (5) $\rho = 0.65\rho_0$, (6) $\rho = 0.86\rho_0$, (7) $\rho = \rho_0[\rho_0 = (1.1 \pm 0.3) \times 10^7$ photons $cm^{-2}\ s^{-1}]$. The lines represent the best fitting of Eq. (1) to the experimental points. From Ref. [2], used with permission, 2000 Elsevier.

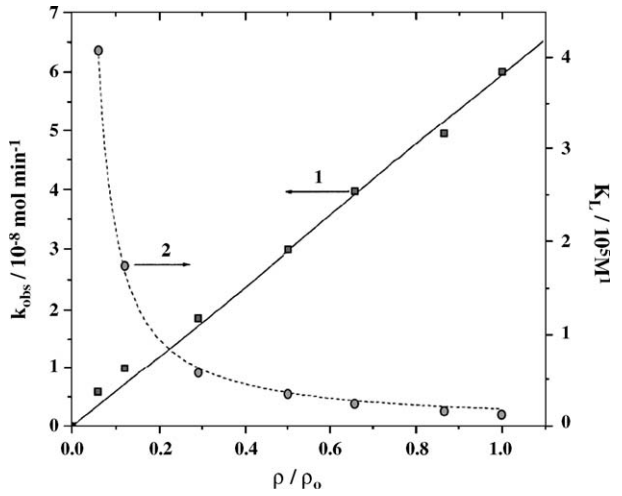

Fig. 3. Dependence on the relative photon flux of actinic light at 365 nm, according to the fitting of Eq. (1) experimental points of Fig. 2 of (a) rate constant, k_{obs}; (b) Langmuir constant, K_L. From Ref. [2], used with permission, 2000 Elsevier.

Eq. (2) is not fulfilled for high enough values of ρ and C. Furthermore, the slope (β/α) is seen to depend on the photon flux, against Emeline et al. assumption that α and β are photon flux independent [2]. Even if (β/α) is apparently constant for curves 1–4 (i.e., for $\rho \leq 5.5 \times 10^{16}$ cm^{-2} s^{-1}), it clearly increases for higher photon fluxes (curves 5–7). This behavior is linked to that observed in Fig. 4, i.e., the apparent deviation from linearity of the plot of K_L^{-1} vs. ρ/ρ_0 for $\rho \geq 5.5 \times 10^{16}$ cm^{-2} s^{-1}. A further analysis of the lack of congruency between Eq. (3) and Emeline et al. experimental results will be performed in the next section.

The phenol photodegradation rate dependence on the photon flux observed by Emeline et al. for different phenol concentrations is reproduced in Fig. 6. According to Eq. (2), for high enough values of C, dC/dt should depend linearly on ρ/ρ_0, a behavior that is not observed for $c \leq 0.851$ mM. Furthermore, according to Eq. (3), the plot of rate^{-1} vs. ρ_0/ρ shown in Fig. 7 should be linear, with a slope γ/α and an intercept of $(\beta/\alpha)(1/C)$. However, it can be observed that, in fact, the expected linearity takes place for low enough phenol concentration values, although a clear slope change (inflection point) appears for $C > 0.638$ mM and $\rho_0/\rho < 3.45$ (i.e., $\rho \geq 3.2 \times 10^{16}$ cm^{-2} s^{-1}), within the range of photon flux and concentration values where the linearity of $(dC/dt)^{-1}$ vs. C^{-1} predicted by Eq. (3) is lost in Fig. 5. This constitutes a further

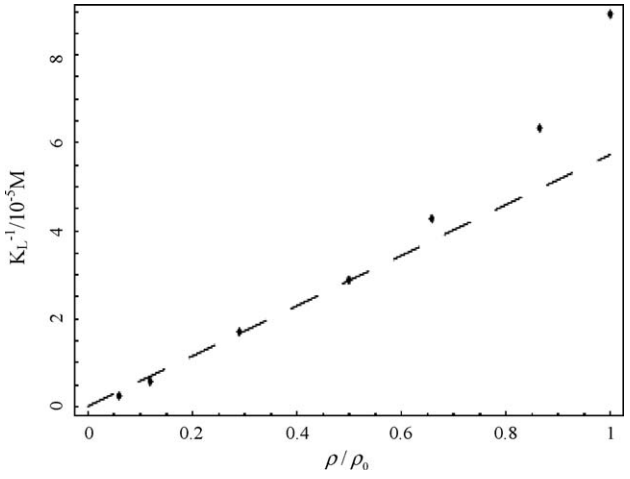

Fig. 4. Dependence of $(K_L)^{-1}$ on ρ/ρ_0 obtained from K_L vs. ρ/ρ_0 plot of Fig. 3.

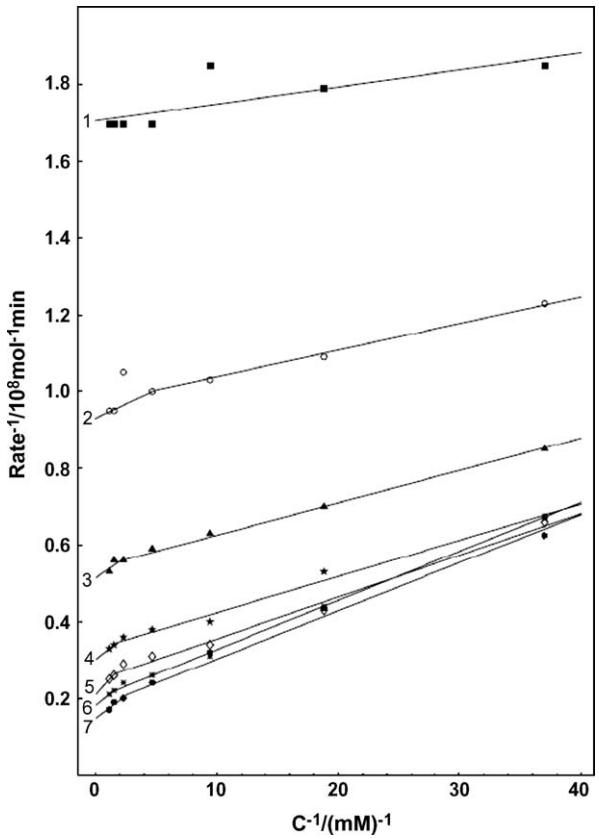

Fig. 5. Dependence of the inverse of the initial rate on the inverse of the concentration obtained from experimental data of Fig. 2. (1) $\rho = 0.06\rho_0$, (2)$\rho = 0.12\rho_0$, (3) $\rho = 0.29\rho_0$, (4) $\rho = 0.50\rho_0$, (5) $\rho = 0.65\rho_0$, (6) $\rho = 0.86\rho_0$, (7) $\rho = \rho_0$[$\rho_0 = (1.1 \pm 0.3) \times 10^7$ photons cm^{-2} s^{-1}].

indication that Eq. (2) does not fit the observed photooxidation rate dependence on phenol concentration and photon flux in the whole experimental range of ρ and C values.

Finally, Emeline et al. assumes that, in general, the phenol photodegradation rate dependence on ρ can be approximated by

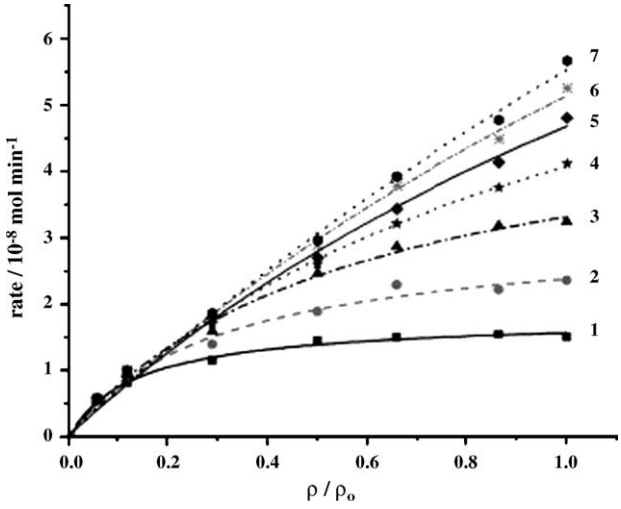

Fig. 6. Initial phenol photodegradation rate dependence on the photon flux of actinic light at 365 nm at different phenol concentrations: (1) $C = 0.027$ mM, (2) $C = 0.053$ mM, (3) $C = 0.106$ mM, (4) $C = 0.213$ mM, (5) $C = 0.427$ mM, (6) $C = 0.638$ mM, and (7) $C = 0.851$ mM. The lines represent the fitting of Eq. (1) to experimental points. From Ref. [2], used with permission, 2000 Elsevier.

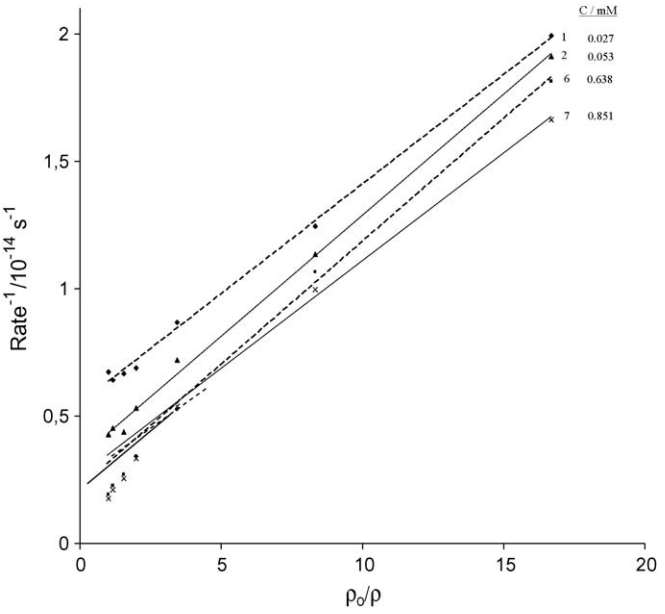

Fig. 7. Plot of the inverse of the rate vs. the inverse of the relative photon flux, from experimental points of Fig. 6.

the expression [2]:

$$\frac{dC}{dt}(\rho) = \frac{ab\rho}{1+b\rho} \tag{4}$$

where the parameters a and b are independent on the photon flux. Obviously, Eqs. (4) and (2) should be equivalent, provided that $a \propto C$ and $b \propto C^{-1}$ if $k_{obs} \propto \rho$ and $K_L \propto \rho^{-1}$, as in fact verified by the authors (see Fig. 4 of Ref. [2]). Under these assumptions, the phenol photodegradation rate dependence on ρ and C may be generalized by Eq. (2). However, given that the condition $K_L \propto \rho^{-1}$ is not fulfilled, as was shown in Fig. 4, Eq. (2) cannot be considered to be a generalized expression of the phenol photodegradation rate dependence on ρ and C.

Summing up, a careful analysis of phenol photodegradation experimental data by Emeline et al. shows that the modified L–H Eqs. (3) and (4) are not congruent with the observed dependence of dC/dt on ρ and C.

3. Testing the direct-indirect (D–I) model via phenol photooxidation experimental data by Emeline et al.

In the absence of specific adsorption the IT mechanism of the D–I model must apply to the photocatalytic oxidation of dissolved substrate species. The photooxidation process can therefore be described by the following sequence of primary interfacial reactions [10], schematized in Fig. 8.

3.1. Charge–carrier generation

$$TiO_2 + h\nu \xrightarrow{\nu'_0} h_f^+ + e_f^-, \qquad \nu'_0 = k'_0\rho \tag{5}$$

where h_f^+ and e_f^- representing photogenerated VB free holes and CB free electrons, respectively.

3.2. Inelastic trapping of VB free holes

There exist an important controversy in TiO_2 photocatalysis about the nature of photogenerated, primary oxidant species. Recently, one of us has shown experimental evidence that filled energy levels of hydroxyl groups bound on terminal Ti ions (OH_{ads}^-)

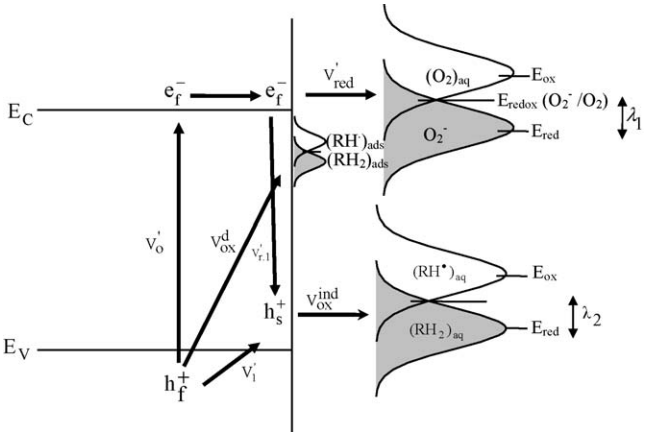

Fig. 8. Diagram showing TiO_2 energy levels and primary interfacial reactions according to which dissolved O_2 molecules are reduced with CB electrons and dissolved RH_2 species (in our case phenol molecules) are photooxidized mainly with surface trapped holes, via an adiabatic IT mechanism. Photooxidation of specifically adsorbed $(RH_2)_{ads}$ substrate species with VB free holes, via an inelastic, DT mechanism is also considered. h_s^+ surface trapped holes should be identified with O_s^- radicals (i.e., holes trapped at terminal oxygen ions), as adsorbed hydroxyl groups cannot be photooxidized with VB holes [13].

are below the VB edge, indicating that their photooxidation with h_f^+ to produce $OH_{ads}^\bullet$ radicals is thermodynamically hindered [13]. Two types of h_f^+ traps exist at the TiO_2 surface with energies above the VB edge: those associated with terminal oxygen ions (O_s^{2-}), at basic pH, which can be photooxidized to O_s^- radicals according to reaction (6):

$$h_f^+ + O_s^{2-} \xrightarrow{\nu'_1} O_s^-(h_s^+), \qquad \nu'_1 = k'_1[h_f^+][O_s^{2-}] \tag{6}$$

and those associated with terminal hydroxyl groups of acidic character resulting from the protonation of terminal O_s^{2-} ions at acidic pH ($O_s^{2-} + H_{aq}^+ \rightarrow OH_s^-$), which are photooxidized to terminal hydroxyl radicals according to reaction (7):

$$h_f^+ + OH_s^- \xrightarrow{\nu'_1} OH_s^\bullet(h_s^+), \qquad \nu'_1 = k'_1[h_f^+][OH_s^-] \tag{7}$$

Both O_s^- and $OH_s^\bullet$ radicals are considered to be surface trapped holes (h_s^+) [13].

3.3. Inelastic charge–carrier recombination

$$h_s^+ + e_f^- \xrightarrow{\nu'_{r,1}} O_s^{2-}, OH_s^-; \qquad \nu'_{r,1} = k'_{r,1}[e_f^-][h_s^+] \tag{8}$$

3.4. Adiabatic interfacial charge transfer

$$e_f^- + (O_2)_{aq} + 2H_{aq}^+ \xrightarrow{\nu'_{red}} (O_2^-)_{aq}, \qquad \nu'_{red} = k'_{red}[e_f^-][O_2]_{aq} \tag{9}$$

$$h_s^+ + (RH_2)_{aq} \xrightarrow{\nu^{ind}_{ox}} RH^\bullet + H_{aq}^+, \qquad \nu^{ind}_{ox} = k^{ind}_{ox}[h_s^+][RH_2]_{aq} \tag{10}$$

$$(O_2^-)_{aq} + 2H_{aq}^+ + 2e_f^- \xrightarrow{\nu'_{red_1}} OH_{aq}^\bullet + OH_{aq}^-, \quad \nu'_{red_1} = k'_{red_1}[e_f^-][O_2^-]_{aq} \tag{11}$$

$$OH_{aq}^\bullet + (RH_2)_{aq} \xrightarrow{\nu_{ox_1}} RH_{aq}^\bullet + H_2O, \qquad \nu_{ox_1} = k_{ox_1}[OH_{aq}^\bullet][RH_2]_{aq} \tag{12}$$

$$e_f^- + RH_{aq}^\bullet + H^+ \xrightarrow{\nu_{back}} (RH_2)_{aq}, \qquad \nu_{back} = k_{back}[e_f^-][RH^\bullet] \tag{13}$$

where $(RH_2)_{aq}$ represents in general solute organic species (phenol in our case), $RH^{\bullet}_{aq}$ are the corresponding photogenerated radicals (phenoxyl radicals in our case), the sub-index "aq" indicating aqueous dissolved species. Reactions (9) and (10) correspond to interfacial transfer of free CB electrons and VB holes to the electrolyte, to produce superoxide and phenoxyl radicals, respectively. Reaction (11) represents the photogeneration of dissolved (non-specifically adsorbed) $OH^{\bullet}_{aq}$ radicals from the electroreduction of photogenerated superoxide radicals. Phenoxyl radicals not only can be photogenerated via reaction (10) but via reaction (12) with intervention $OH^{\bullet}_{aq}$ radicals photogenerated according to (11). Finally, reaction (13) represents the back reaction of (10). According to this mechanistic scheme, $d[RH_2]_{aq}/dt = \nu_{ox}^{ind} + \nu_{ox_1} - \nu_{back}$. However, when initial photooxidation rates are considered, as it is the case for the phenol photooxidation study by Emeline et al. [2], it can be assumed that $\nu_{ox}^{ind} \gg \nu_{ox_1}, \nu_{back}$, since for $t \to 0$ the concentration of both $OH^{\bullet}_{aq}$ and $RH^{\bullet}_{aq}$ radicals is negligible with respect to the concentration of surface trapped holes (h_s^+); therefore it can be considered that $\lim_{t\to 0}(d[RH_2]_{aq}/dt) \approx \nu_{ox}^{ind}$.

It is worth noting that under pseudo-steady state conditions $\nu'_{red} = \nu_{ox}^{ind}$, which means that the flux of CB electrons and VB holes from the semiconductor to the electrolyte must be identical, as the principle of semiconductor electroneutrality conservation must be preserved. On the other hand, the compatibility of Emeline et al. E–R kinetics with Eq. (2) is a consequence of assuming that the electron–hole recombination rate depends linearly on the photon flux (see Eq. (27b) of ref. [2]), an assumption that is not compatible with the IT mechanism [9]. This is the reason why both models lead to different kinetic expressions. In fact, according to the preceding simplified reaction scheme, the initial phenol photooxidation rate dependence on the photon flux and phenol concentration under pseudo-steady state conditions, is given by [10]:

$$\frac{dC}{dt} \approx \nu_{ox}^{ind} = \left[(aC)^2 + 2ak'_0\rho C\right]^{1/2} - aC \qquad (14)$$

where $a = (k_{ox}^{ind}k'_{red}[O_2]_{aq})/4k'_{r,1}$ (cm s^{-1}) and C and ρ are expressed in cm^{-3} and $cm^{-2}\,s^{-1}$, respectively. According to (14), the photooxidation quantum yield approaches unity as $\rho \to 0$, but decreases as ρ increases [9,10]. This is due to the fact that even if both ν_{ox}^{ind} and $\nu'_{r,1}$ increase with the photon flux, the increase of the recombination rate ($\nu'_{r,1}$) is higher than the increase of ν_{ox}^{ind}, so that $\nu_{ox}^{ind}/\nu'_{r,1}$ decreases as ρ increases. In cases where the actual activated surface area of the catalyst in the reactor, (A), is known, Eq. (14) can be substituted by Eq. (15), which represents the observed photooxidation rate expressed in s^{-1} and not in $cm^{-2}\,s^{-1}$, as it was in Eq. (14):

$$\left(\frac{dC}{dt}\right)_{obs} = \left[(a_{obs}C)^2 + 2a_{obs}b\rho C\right]^{1/2} - a_{obs}C \qquad (15)$$

where $b = Ak'_0$, expressed in cm^2, is a constant and $a_{obs} = Aa$. Since the experimental data by Emeline et al. [2] do not include the values of A and k'_0, they have to be analyzed in terms of Eq. (14). Importantly, note that in contrast with Eq. (1), Eq. (14) does not predict a linear dependence of the inverse of $(dC/dt)^{-1}$ on C^{-1}. On the other hand, the physical meaningless parameters α, β and γ of Eq. (2) are substituted in Eq. (14) by the parameter a, which has a well defined physical meaning.

From diverse assumptions and alternative photooxidation mechanisms, rate equations similar to Eq. (14) have been obtained by different authors [11,67,68]. However, these approaches were not based on the degree of interaction of dissolved substrate species with the semiconductor surface and on the nature of interfacial charge transfer mechanisms, as done by the D–I model.

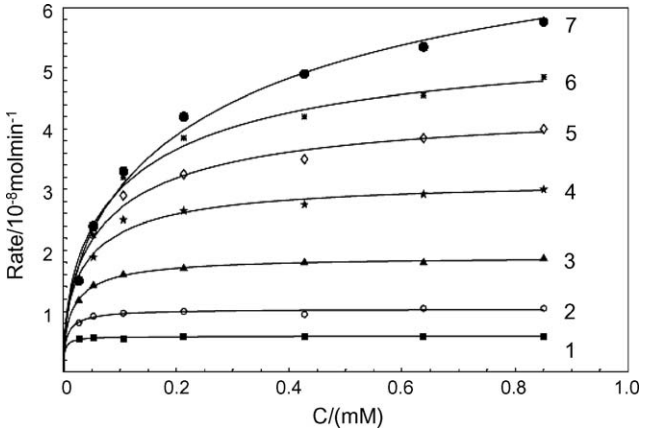

Fig. 9. Fitting of Eq. (14) to experimental points of Fig. 2.

The fitting of Eq. (14) to the experimental plots by Emeline et al. [2], for constant ρ, of rate vs. C (Fig. 2), $rate^{-1}$ vs. C^{-1} (Fig. 5), rate vs. ρ (Fig. 6) and $rate^{-1}$ vs. ρ^{-1} for C = constant (Fig. 7) are shown in Figs. 9–12, respectively. Specially interesting is the fitting of Eq. (14) to the plot of $rate^{-1}$ vs. C^{-1}, shown in Fig. 10. Note that, in contrast to Eq. (2), this fitting is good even for high enough values of C and ρ. Fitting curves were obtained in general for values of the parameter a represented in Fig. 13 as a function of C and ρ. Because of the lack of experimental information on the characteristics of the reactor used by Emeline et al. [2] we assume that $k'_0 = 1$ in Eq. (5). Although the values of a in Fig. 13 are not exact (they depend on the actual value of k'_0 and A), the observed dependence of a on C and ρ is not affected by the value assumed for k'_0.

It was assumed in a previous publication that the parameter a does not depend on C and ρ [10]. This assumption was made on the

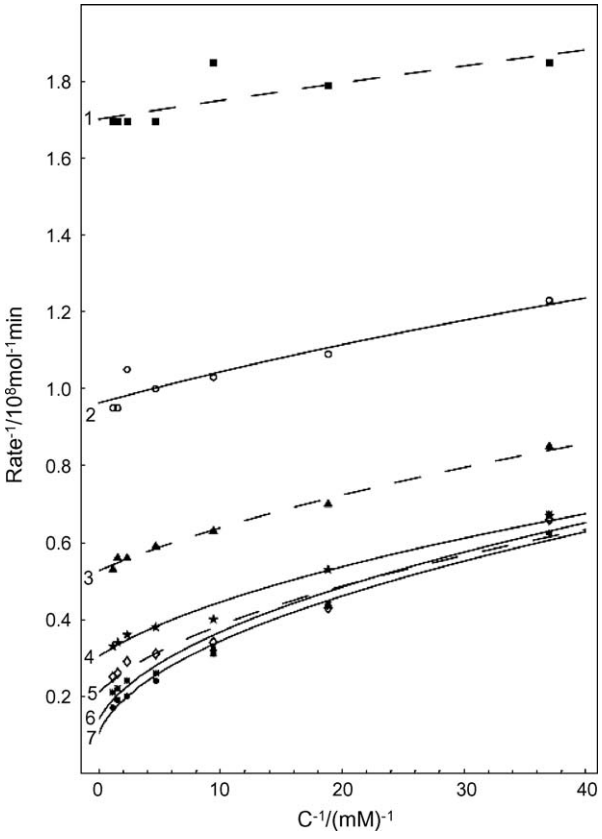

Fig. 10. Fitting of Eq. (14) to experimental points of Fig. 5.

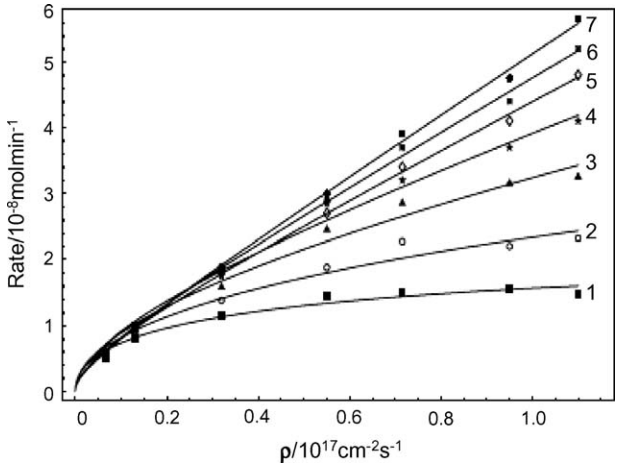

Fig. 11. Fitting of Eq. (14) to experimental points of Fig. 6.

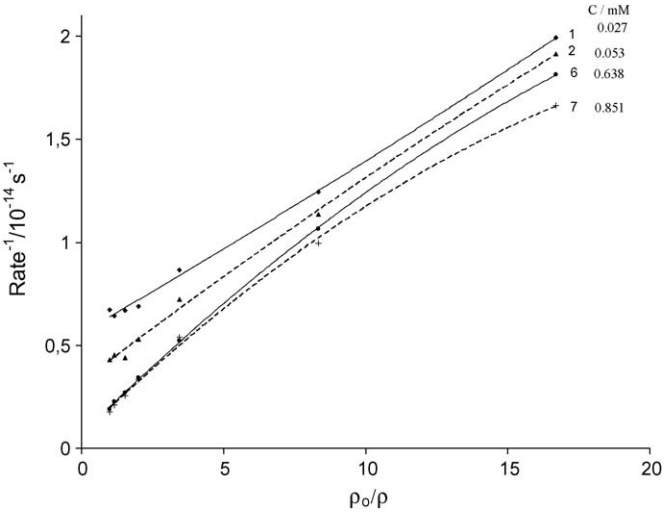

Fig. 12. Fitting of Eq. (14) to experimental points of Fig. 7.

basis that the energy levels of the semiconductor (E_C, E_V, $E(h_s^+)$, etc.) are not influenced by C and ρ. However, the results of Fig. 13 seem to contradict this hypothesis. On the one hand, both a and $(da/d\rho)$ apparently decreases as C increases; on the other hand, for low

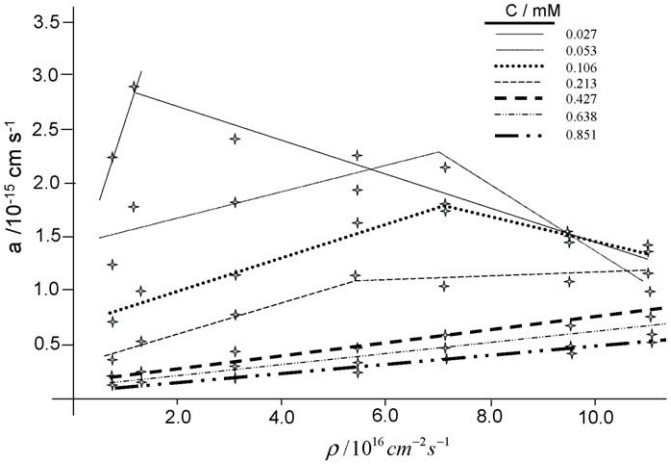

Fig. 13. Dependence of parameter a in Eq. (14) on photon flux and phenol concentration, obtained from the fitting of Eq. (14) to experimental data by Emeline et al. [2] in Fig. 5.

enough C values ($C \leq 0.1$ mM) $a(\rho)$ presents a maximum, while for high enough C values ($C \geq 0.4$ mM) a monotonous increase of a with ρ is observed in the full experimental range of ρ ($5 \times 10^{15} < \rho < 10^{17}$ cm^{-2} s^{-1}) and the maximum does not appear. In order to rationalize this observed behavior two hypothesis can be formulated: (a) a change of both the rate constants k'_{red} and k_{ox}^{ind} which, according to the Marcus–Gerischer fluctuating energy model for adiabatic transfer of charge at the sc–electrolyte interface under weak semiconductor–substrate interaction [69], depend on the degree of overlapping between semiconductor and electrolyte energy levels (see Fig. 8), as

$$k'_{red} \propto \exp\left[-\frac{(E_{ox}(O_2) - E_C)^2}{4\lambda_1 kT}\right] \quad (15')$$

and

$$k_{ox}^{ind} \propto \exp\left[-\frac{(E_{red}(RH_2) - E(h_s^+))^2}{4\lambda_2 kT}\right], \quad (15'')$$

where $E(h_s^+)$ is the energy of surface trapped holes and λ the reorganization energy. Since the values of $(E_{red}(RH_2) - E(h_s^+))$ and $(E_{ox}(O_2) - E_C)$ are sensitive to the actual surface concentration of trapped electrons and holes, $[h_s^+]$ [70], both depending on C and ρ, a dependence of k'_{red} and k_{ox}^{ind} on photon flux and substrate concentration may be expected; (b) we have considered that interfacial hole transfer during phenol photooxidation is exclusively due to an adiabatic IT mechanism (Eq. (14)), as no specific adsorption with the TiO_2 surface exist. However, the existence of electronic interaction, even if small, of dissolved phenol species with the semiconductor surface would produce the intervention of VB free holes via an inelastic DT mechanism in phenol oxidation. Consequently, Eq. (14) should be substituted by Eq. (19) of the next section, which takes into account the simultaneous intervention of both DT and IT mechanism. Under weak specific adsorption of phenol species, the photooxidation rate dependence on C and ρ expressed by Eq. (19) should be very close to that expressed by Eq. (14), resulting in a new expression where the parameter a apparently depends on the photon flux and concentration as appear in Fig. 13. These considerations will be analyzed in detail in a further publication.

4. Formic acid photooxidation: a kinetic reanalysis of literature experimental data to the light of the D–I model

HCOOH is an aliphatic compound that is photooxidized to CO_2 and H_2O following a single mechanism, without formation of intermediate products or multiple reactions; this is the reason why FA has been selected by different authors as a prove photodegradation reaction [15,71–73].

From the ATR-IR experimental results of Fig. 1, FA appears to be specifically adsorbed on TiO_2 in the presence of water. According to the D–I model, this means that for high enough illumination flux (within the usual experimental range) both mechanisms IT and DT coexist in FA photodegradation, as schematized in the energy diagram of Fig. 8. Therefore, reactions (16)–(18) are considered to take place simultaneously to reactions (10)–(12) [10]:

$$(RH_2)_{ads} + h_f^+ \xrightarrow{\nu_{ox}^d} RH^\bullet + H^+ \quad (16)$$

$$RH^\bullet + h_f \xrightarrow{\nu_{ox}^{d,2}} R + H_{aq}^+ \quad (17)$$

$$RH^\bullet + H^+ + e_f^- \xrightarrow{\nu_{back}} (RH_2)_{ads} \quad (18)$$

where $(RH_2)_{ads}$ concerns specifically adsorbed FA species. As for reaction (13), reaction (18) can be omitted when, as usual, the

kinetic analysis considers initial photooxidation rates. Furthermore, because of the high overlapping between filled energy levels of photogenerated HCOO radical species and CB empty levels, which is the cause of the observed "current doubling" phenomenon [75], v_{back} is negligible even for high illumination times. On the other hand, as pointed out in Section 3, the participation of free (non-adsorbed) OH radicals generated from oxygen electroreduction at the beginning (first instants) of the photooxidation process can be omitted as their photogeneration rate is negligible by comparison with the generation rate of VB free holes and surface trapped holes. Furthermore, hydrogen peroxide, generated as an intermediate species in reaction (11), is not able to oxidize FA [14]. Under these conditions the photooxidation rate can be expressed by Eq. (19) [9,10]:

$$\frac{dC}{dt} = v_{ox}^{d} + v_{ox}^{ind} = \frac{k_{ox}^{d}[(RH_2)_{ads}]\rho}{k_1'[O_s^{2-}] + k_{ox}^{d}[(RH_2)_{ads}]} + [(aC)^2 + 2ak_0'\rho C]^{1/2} - aC \quad (19)$$

where the concentration of specifically adsorbed FA species is approached by a Langmuir type adsorption isotherm:

$$[(RH_2)_{ads}] = \frac{AB[(RH_2)_{aq}]}{1 + A[(RH_2)_{aq}]} \quad (20)$$

A and B being the adsorption constant and the surface concentration of adsorption sites, respectively. By combining (19) and (20) for $v_{ox}^{d} \gg v_{ox}^{ind}$ (i.e., for DT prevailing on IT), as we will show below to be the case for FA, the photooxidation rate becomes:

$$\frac{dC}{dt} \approx v_{ox}^{d} = \frac{k_{ox}^{d}AB[(RH_2)_{aq}]\rho}{k_{ox}^{d}AB[(RH_2)_{aq}] + k_1'[O_s^{2-}](1 + A[(RH_2)_{aq}])} \quad (21)$$

Eq. (21) predicts a photon flux linearly dependent photooxidation rate and, therefore, an independent photooxidation quantum yield. In principle, the D–I model considers that the adsorption–desorption equilibrium existing in the dark is not broken under illumination. However, when non-equilibrated adsorption of reactants is assumed to take place under illumination, the photodegradation rate no longer depends linearly on the photon flux [10].

Fig. 14 reproduces the plot of formic acid photodegradation rate ($R^{(0)}$) vs. the volume-average square root of the photon flux ($G_a^{1/2}$), experimentally obtained by Davydov and Smirnotis [14]. Although the authors do not indicate the solution pH used in the experiments, it may be assumed that a pH < 4.0 was used, as formate ions do not adsorb significantly on the TiO_2 surface above

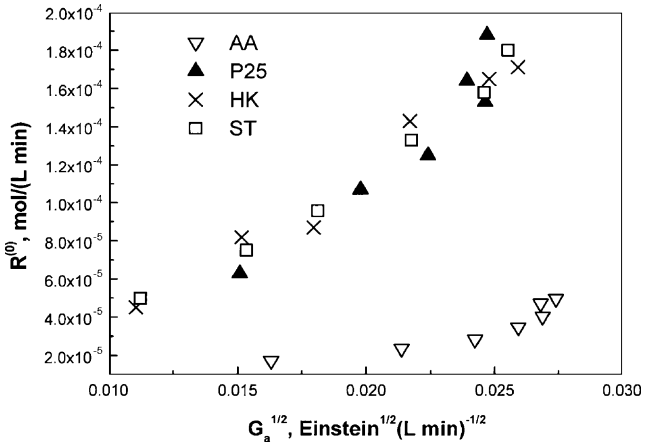

Fig. 14. Formic acid photodegradation rate dependence on the photon flux square root, under UV illumination of a 450-W (medium-pressure) mercury vapour quartz lamp, for a FA initial concentration 30 mM and four different TiO_2 samples (AA, P25, HX and ST). From Ref. [14], used with permission, 2000 Academic Press.

pH 4.0 [74]. Note that the coordinates origin ($R^{(0)} = 0$ for $G_a = 0$) was omitted by the authors. Probably influenced by the general believe that $R^{(0)} \propto G_a^n$, with $n = 1$ and 1/2 for low and high photon flux, respectively [76–78]. In fact, Davydov and Smirnotis claim that the plot of $R^{(0)}$ vs. $G_a^{1/2}$ is linear. However, as can be seen in Fig. 15, when the coordinate's origin is included in the plot, evidence is obtained that the photooxidation rate does not depend linearly on the square root of the photon flux but on the photon flux, as also obtained by Buechler et al. [74]. This linear dependence of the photooxidation rate on the photon flux seems to contradict the claim that under high enough illumination intensity the photooxidation rate should be proportional to the square root of the photon flux [77–79]. In contrast, this is just the behavior predicted by the D–I model (Eq. (21)) for specific adsorption, at any photon flux, when DT prevails on IT under adsorption–desorption equilibrium conditions [9,10]. The same linear dependence has been reported for acetic acid [79], another aliphatic compound prone to be adsorbed on TiO_2 in aqueous medium. It must be noted that a linear dependence of the photooxidation rate on the photon flux is also predicted by Eq. (2), but only in the limit case that $(\rho/C) << (\gamma/\beta)$ (i.e., for low enough ρ and high enough C), a limitation non existing in the D–I model. However, it is inferred from experimental data of Fig. 15 that $(\rho/C) \approx (\gamma/\beta)$ for $\rho \geq 6 \times 10^{-4}$ Einsein/L min, so that it can be stated that Eq. (2)

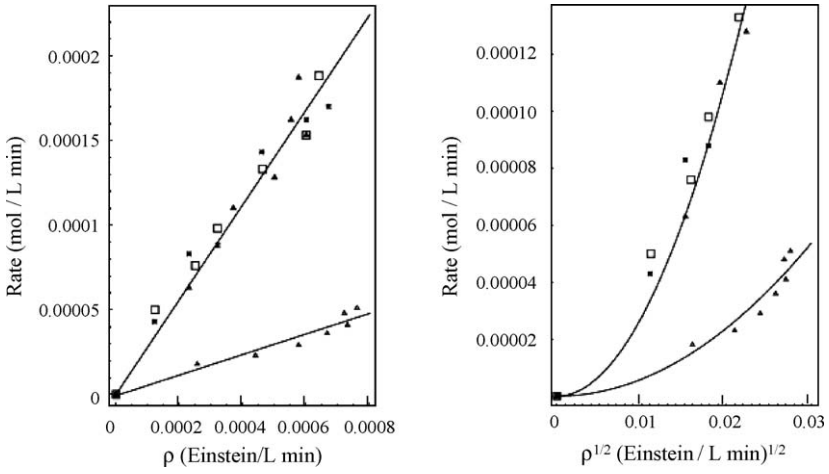

Fig. 15. Formic acid photooxidation rate plots on: (a) photon flux and (b) square root of photon flux, from experimental data of Fig. 14.

is not coherent with FA photooxidation kinetic data obtained from Fig. 15. Further experimental evidence about this conclusion will be published elsewhere.

5. Conclusions

Experimental evidence has been shown that while phenol molecules in aqueous solution are scarcely adsorbed on TiO_2, dissolved formic acid efficiently competes with water species for being bound to terminal Ti atoms.

Kinetic data from the literature concerning the illumination intensity and substrate concentration dependence of the photocatalytic oxidation of phenol and formic acid on TiO_2 aqueous dispersions have been reanalyzed in the light of the D–I model. With respect to phenol, the absence of linearity in the plots of the inverse of the photooxidation rate, $(dC/dt)^{-1}$, vs. the inverse of the phenol concentration (C), under high enough photon flux (ρ), and of the inverse of ρ for high enough C, indicates that phenol photooxidation kinetics is not compatible with the behavior predicted by the L–H model. In contrast, as predicted by the D–I model, when IT is the dominant interfacial charge transfer mechanism, a photooxidation rate expression of the type $(dC/dt) = [(aC)^2 + 2a\rho C]^{1/2} - aC$, seems to be compatible with kinetic experimental data, with the parameter a apparently depending on photon flux and phenol concentration, but showing a tendency to become constant as C increase and ρ decreases. This behavior may be attributed to a shift of TiO_2 energy levels with respect to electrolyte levels, because of the accumulation of electrons and holes at the semiconductor surface. However, the influence that the specific adsorption of phenol, even if weak, may have on the apparent dependence of a on ρ and C cannot be neglected.

In contradiction with the behavior predicted by the L–H model, a linear dependence of formic acid photooxidation rate on ρ, for constant C, is found even at high enough values of ρ/C, in the same range where linearity is not observed for phenol. We demonstrate that this is just the behavior predicted by the D–I model under strong specific adsorption of dissolved substrate species, when DT mechanism prevails on IT.

Acknowledgements

Financial support from the Spanish Ministerio de Educación y Ciencia (MEC) through the project CTQ2006-06286/BQU (Fondos FEDER) and from the Generalitat Valenciana (ACOMPO7-095) is acknowledged. We tank R. Gomez, A. Rodes and D. Monllor-Satoca for stimulating discussions and for supplying the ATR-IR spectra shown in Fig. 1.

References

[1] K. Okamoto, Y. Yamamoto, H. Tanaka, A. Itaya, Bull. Chem. Soc. Jpn. 58 (1985) 2023.
[2] A.V. Emeline, V. Riabchuk, N. Serpone, J. Photochem. Photobiol. A: Chem. 133 (2000) 89.
[3] V. Emeline, V. Riabchuk, N. Serpone, J. Phys. Chem. B 109 (2005) 18515.
[4] R.W. Mathew, J. Catal. 111 (1988) 264.
[5] C.S. Turchi, D.F. Ollis, J. Catal. 122 (1990) 1109.
[6] W.Y. Wei, C. Wan, J. Photochem. Photobiol. A: Chem. 69 (1992) 241.
[7] E. Pelizzetti, C. Minero, Electrochim. Acta 38 (1993) 47.
[8] D.F. Ollis, J. Phys. Chem. B 109 (2005) 2439.
[9] T. Lana Villarreal, R. Gomez, M. Gonzalez, P. Salvador, J. Phys. Chem. B 108 (2004) 20278.
[10] D. Monllor-Satoca, R. Gomez, M. Gonzalez-Hidalgo, P. Salvador, Catal. Today 129 (1–2) (2007) 247.
[11] H. Gerischer, Electrochim. Acta 40 (1995) 1277.
[12] S.R. Morrison, Electrochemistry at Semiconductors and Oxidized Metal Electrodes, Plenum Press, New York, 1980.
[13] P. Salvador, J. Phys. Chem. C 111 (2007) 17038.
[14] L. Davydov, P. Smirnotis, J. Catal 191 (2000) 105.
[15] M. Lapertot, P. Pichat, S. Parra, Ch. Guillard, C. Pulgarin, J. Environ. Sci. Health A 41 (2006) 1009.
[16] J. Ryu, W. Choi, Environ. Sci. Technol. 42 (2008) 294.
[17] A. Mills, S. Morris, J. Photochem. Photobiol. A: Chem. 71 (1993) 75.
[18] J. Cunningham, P. Sediák, J. Photochem. Photobiol. A: Chem. 77 (1994) 255.
[19] S. Tunesi, M. Anderson, J. Phys. Chem. 95 (1991) 3399.
[20] K. Okamoto, Y. Yamamoto, H. Tanaka, A. Itaya, Bull. Chem. Soc. Jpn. 58 (1985) 2015.
[21] R.W. Mathews, J. Phys. Chem. 91 (1987) 3328.
[22] L. Palmisano, V. Augugliaro, A. Sclafani, M. Schiavello, J. Phys. Chem. 92 (1988) 6710.
[23] V. Augugliaro, L. Palmisano, A. Sclafani, C. Minero, E. Pelizzetti, Toxicol. Environ. Chem. 92 (1988) 6710.
[24] A. Sclafani, L. Palmisano, M. Schiavello, J. Phys. Chem. 94 (1990) 829.
[25] T.Y. Wei, Y-Y. Wang, C-C. Wang, J. Photochem. Photobiol. A: Chem. 55 (1990) 115.
[26] R.W. Mathews, Water Res. 24 (1990) 653.
[27] A. Sclafani, L. Palmisano, E. Daw, New. J. Chem. 14 (1990) 265.
[28] T. Wei, C. Wang, Ind. Eng. Chem. Res. 30 (1991) 1293.
[29] M. Trillas, J. Peral, X. Domenech, Appl. Catal. B: Environ. 3 (1993) 45.
[30] J. Hermann, G. Guillard, P. Pichat, Catal. Today 17 (1993) 7.
[31] K. Vinodgopal, U. Statford, K.A. Gray, P.V. Kamat, J. Phys. Chem. 98 (1994) 6797.
[32] S. Cheng, S.J. Tsay, Y.F. Lee, Catal. Today 26 (1995) 87.
[33] W. Yizhong, H. Chun, T. Hougxiao, Chemosphere 41 (2000) 1205.
[34] U. Statford, K.A. Gray, P.V. Kamat, Heterogen. Chem. Rev. 3 (1996) 77.
[35] T. Tisler, Zagore-Koncan, J. Water Air Soil Pollut. 97 (1997) 315.
[36] L.J. Alemany, M.A. Bañares, E. Pardo, F. Martin, M. Galan Ferreres, J.M. Blase, Appl. Catal. 13 (1997) 299.
[37] C.B. Mangens, A.A. Kagerman, Water Res. 31 (1997) 3116.
[38] H. Chun, W. Yizhong, T. Hougxiao, Environ. Sci. 18 (1997) 1.
[39] J.A. Byrne, B.R. Eggins, N.M. Brown, B. Mckiney, M. Rouse, Appl. Catal. B: Environ. 17 (1998) 25.
[40] E. Leyva, E. Moctezuma, M.G. Ruiz, L. Torres Martinez, Catal. Today 40 (1998) 367.
[41] V.C. Saha, F. Kaviraj, Bull. Environ. Contam. Toxicol. 63 (1999) 195.
[42] C. Minero, G. Mariella, V. Maurino, E. Pelizzetti, Langmuir 16 (2000) 2632.
[43] C. Minero, G. Mariella, V. Maurino, D. Vione, E. Pelizzetti, Langmuir 16 (2000) 8964.
[44] P. Calza, E. Pelizzetti, Pure Appl. Chem. 73 (2001) 1839.
[45] Ö.E. Kartal, M. Erol, H. Oguz, Chem. Eng. Technol. 24 (2001) 6.
[46] A. Dawson, P.V. Kamat, J. Phys. Chem. B 105 (2001) 960.
[47] A.M. Peioro, J.A. Ayllon, J. Peral, X. Domenech, Appl. Catal. Environ. 30 (2001) 359.
[48] C. Wu, X. Liu, D. Wei, L. Wang, Water Res. 35 (2001) 3927.
[49] M. Anderson, L. Österlund, S. Ljungtröm, A.Q. Palmquist, J. Phys. Chem. B 106 (2002) 1064.
[50] F.B. Li, X.Z. Li, Appl. Catal. A: Gen. 228 (2002) 15.
[51] M. Jacob, H. Levanon, P.V. Kamat, Nano Lett. 3 (2003) 353.
[52] H. Park, W. Choi, J. Phys. Chem. B 108 (2004) 4093.
[53] A. Sobezynski, L. Duczmal, W. Zmudzinski, J. Mol. Catal. A: Chem. 21 (2004) 225.
[54] D. Vione, C. Minero, V. Maurino, M.E. Carlotti, T. Picatonotto, E. Pelizzetti, Appl. Catal. B: Environ. 58 (2005) 81.
[55] F.J. Beltran, F.J. Rivas, O. Gimeno, J. Chem. Technol. Biotechnol. 80 (2005) 973.
[56] Z. Wang, W. Cai, X. Hong, F. Xu, Ch. Cai, Appl. Catal. B: Environ. 57 (2005) 223.
[57] A.G. Agrios, P. Pichat, J. Photochem. Photobiol. A: Chem. 180 (2006) 130.
[58] G. Zhifeng, M. Ruixin, L. Guojun, Chem. Eng. J. 119 (2006) 55.
[59] V. Loddo, M. Addamo, V. Agugliaro, L. Palmisano, M. Schiavello, E. Garrone, AIChE J. 52 (2006) 2565.
[60] T. Amukunprasert, Ch. Saiwan, E. Traversa, J. Mater. Res. 21 (2006) 3001.
[61] C.A. Emilio, M.I. Litter, M. Kunst, M. Bouchard, C. Colbeau-Justin, Langmuir 22 (2006) 3606.
[62] G. Colon, J.M. Sanchez España, M.C. Hidalgo, J.A. Navio, J. Photochem. Photobiol. A: Chem. 179 (2006) 20.
[63] R. Enriquez, A.G. Agrios, P. Pichat, Catal. Today 120 (2007) 196.
[64] A.V. Emeline, X. Zhang, M. Jin, T. Murakami, A. Fujishima, J. Phys. Chem. B 110 (2006) 7409.
[65] Z. Ding, G.Q. Lu, P.F. Greenfield, J. Phys. Chem. B 104 (2000) 4815.
[66] S. Horikoshi, H. Hidaka, N. Serpone, Chem. Phys. Lett. 376 (2003) 475.
[67] C. Minero, Catal. Today 54 (1999) 205.
[68] I.N. Martyanov, E.N. Savinov, J. Photochem. Photobiol. A: Chem. 134 (2000) 219.
[69] H. Gerischer, Surf. Sci. 18 (1969) 97.
[70] P. Salvador, J. Phys. Chem. 89 (1985) 3863.
[71] C.J.G. Cornu, A.J. Colussi, M.R. Hoffmann, J. Phys. Chem. B 105 (2001) 1351.
[72] M.F.J. Dijkstra, H.J. Panneman, J.G.M. Winkelman, J.J. Kelly, Chem. Eng. Sci. 57 (2002) 4895.
[73] M. Mrowetz, E. Selli, New J. Chem. 30 (2006) 108.
[74] K. Buechler, C. Nam, T. Wawistowski, R. Noble, C. Koval, IEC Res. 38 (1999) 1268.
[75] T. Lana-Villarreal, R. Gomez, M. Neumann-Spallart, N. Alonso-Vante, P. Salvador, J. Phys. Chem. B 108 (2004) 15172.
[76] D.F. Ollis, E. Pellizzetti, N. Serpone, Environ. Sci. Technol. 25 (1991) 1522.
[77] J.C. D'Oliveira, G. Al-Sayed, P. Pichat, Environ. Sci. Technol. 24 (1990) 990.
[78] S. Brosillon, L. Lhomme, C. Vallet, A. Bouzaza, D. Wolbert, Appl. Catal. B: Environ. 78 (2008) 232.
[79] M. Bideau, B. Claudel, L. Faure, Y.H. kazouan, J. Photochem. Photobiol. A: Chem. 61 (1991) 269.
[80] H. Günzler, H.-U. Gremlich, IR Spectroscopy. An Introduction, Wiley–VCH, 2002.